Environ Geol (2007) 52:385–397
DOI 10.1007/s00254-006-0588-3

ORIGINAL ARTICLE

Mineralogical, geochemical and microfabric evidences of gypsum crusts: a case study from Budapest

Siegfried Siegesmund · Akos Török · Andre Hüpers · Christian Müller · Werner Klemm

Received: 1 August 2006 / Accepted: 22 November 2006 / Published online: 14 December 2006

Abstract High levels of SO_2 and particulate pollution enable the rapid development of gypsum-rich weathering crusts in Budapest. Two types of white crusts, thin and thick ones, and two forms of black crusts, laminar and framboidal ones, were studied in limestone buildings of the parliament and Citadella. The percentage of crust cover and damage categories were documented on selected walls. Petrographic, XRD, XRF and sulphur isotope analyses were performed under laboratory conditions to understand the mechanism of crust formation. White crusts found both on exposed and sheltered walls display a calcite-rich layer with gypsum, while black crusts are enriched with gypsum. The sulphur isotopic composition of white and black crusts overlaps, but the crusts are slightly enriched in heavy isotopes compared to rainwater. S content, Si/Al ratios and particulates in black crusts suggest that air pollution (SO_2, dust) contributes to black crust formation. The accumulation of sulphur and Zn enrichment of white crusts were also documented indicating that under high pollution levels, even these compound can accumulate on exposed facades.

Keywords Air pollution · Weathering crust · Gypsum · Geochemistry · Limestone

S. Siegesmund (✉) · A. Hüpers · C. Müller
Geoscience Centre, University of Göttingen,
Goldschmidtstr. 3, 37077 Göttingen, Germany
e-mail: ssieges@gwdg.de

A. Török
Department of Construction Materials and Engineering Geology, Budapest University, Sztoczek u. 2,
1111 Budapest, Hungary

W. Klemm
Institute for Mineralogy, Technical University Bergakademie Freiberg, Brennhausgasse 14,
09596 Freiberg, Germany

Introduction

The cultural heritage of Budapest includes many stone buildings and monuments, which were constructed with limestone. Limestone is particularly prone to air pollution related deterioration of dimension stones and stone ornaments. The formation of weathering crusts has been debated for a long time and was reported from all over the world (e.g. Kieslinger 1932; Winkler 1970). This phenomenon is mostly ascribed to the transformation of calcium carbonate into calcium sulphate. It is generally accepted that rapid industrialization and urbanization had caused a significant increase of air pollutant concentration in the atmosphere, especially of gaseous and particulate sulphurous compounds. The total amount of anthropogenic sulphur may be absorbed by the building stones themselves or by binder materials, aggregates or rising water, etc. In consequence, the formation of gypsum crusts may cause significant decay with, often, catastrophic results. More recently, pollution has changed to a multi-pollutant situation due to a significant decrease of SO_2.

In Budapest (Hungary), there are many examples of historic buildings, constructed of oolitic limestone, that were exposed to high pollution conditions in the past. Ashlars of the Parliament and Citadella were studied

to assess the processes of atmospheric pollution related decay of porous limestone and freshwater limestone. Different types of weathering crusts cover most parts of the buildings. White crusts (thin and thick laminar) and black crusts (laminar and framboidal) are the most frequent decay features. The detachment of the crusts is characterized by contour scaling, multiple flaking or blistering that may lead to accelerated decay of the substrate; i.e. crust removal is followed by granular disintegration. Alternatively, secondary crust formation prevailing within the first few centimeters may temporarily stabilize the stone surface. Detailed mapping of deterioration features enabled us to quantify the percentage of each weathering form. Biological action, enhanced by the air pollution, may also contribute to the weathering.

The development and frequency of weathering crusts were studied in the field and in the laboratory. The investigation indicates a close relationship between the air pollutants and crust development. As part of a more extended study on the decay problems of the oolithic limestone in urban areas, we have combined the on-site characterization of the decay features also as function of the exposition with respect to the relationship between changes in mineralogical/geochemical composition and surface properties. The comparison of the different crusts, considering the mineralogy, chemistry and sulphur isotopic composition, may help to explain the complex process of sulphate formation with respect to the mineralogical composition and rock fabric of the host rock.

Environment and limestones

The studied buildings are located in different parts of Budapest, a city with a population of nearly 2 million. Thus, besides a continental climate, these monuments are also exposed to air pollution and suffer from anthropogenic effects. The annual mean temperature is 11°C but winter frosts are common, and the number of annual freeze-thaw cycles is on an average 78 (Fig. 1a). The relative humidity shows diurnal and annual changes with lower values in the morning and increased values in the evening with a yearly maximum of nearly 90% during winter (Fig. 1b). The main gaseous pollutants are NO_x and SO_2, but air quality has improved with respect to SO_2 in the past decade (Fig. 1c). After a period of decline in the amount of settling dust, a recent increase has been recorded. Heavy urban traffic is the main source of SO_2, NO_x and settling dusts. The distribution of pollutants is uneven, since the city centre, where street canyons and several storey buildings are found, experiences nearly 50% of the pollution (Fig. 1d, e).

The studied buildings were mostly built of miocene porous limestone. This limestone was a popular building stone at the end of the nineteenth century and the beginning of the twentieth century. The Citadella (Fig. 2a) was almost entirely constructed of miocene limestone, while in the Parliament building (Fig. 2b) the historic porous limestone ashlars are being replaced by travertine during the current restoration works. Miocene porous limestone was also used for the construction of the Budapest Opera House and the Mathias Church (Török 2002). This white-yellowish grainstone derives from nearby quarries in the vicinity of Budapest (Sóskút, Kõbánya, Budafok, Nagytétény). The main components are well to moderately rounded ooids and micro-oncoids. Other calcitic components have been described as fragments of red algae, gastropods, bivalves and foraminifera (Török and Rozgonyi 2004). Idiomorphic microsparite crystals provide the cement of the grainstones. Quartz and feldspar are the accessory minerals and are often visible as cores of the ooids. The porosity is high with values of more than 30% (Hüpers et al. 2005).

A lithological mapping at the Parliament building and the Citadella fortress showed that textural elements show variations in their size and frequency. Three lithotypes were identified: coarse-grained, medium-grained and fine-grained limestone.

The coarse-grained limestone encompasses carbonate grains of 0.4–5 mm in size. Non-carbonate compounds such as small quartz grains and lithic clasts also occur (Fig. 3a). The texture is grain supported with more biogenic material (shell fragments, gastropods, foraminifera, etc.) and microbial (ooids, micro-oncoids, etc.) than inorganic compounds such as terrigenious quartz and feldspar. The microsparitic cement has a contribution of ca. 15 vol% (Fig. 3b).

The average grain size of the medium-grained limestone is 0.5 mm (Fig. 3c). This lithotype is grain supported with a higher amount of biogenic components (ca. 60 vol%) and a minor microsparitic cement (≤5 vol%). The main carbonate constituents are ooids, foraminifera, gastropods and shell fragments (Fig. 3d).

The fine-grained limestone has a uniform grain supported texture with a relatively high proportion of microsparite (40–60 vol%). The amount of inorganic and biogenic components is 10–20 vol% with an average grain size of 0.2 mm. Biogenic components include foraminifera and shell fragments (Fig. 3e, f).

Besides miocene limestone, the Pliocene–Pleistocene travertine has also been a popular building stone

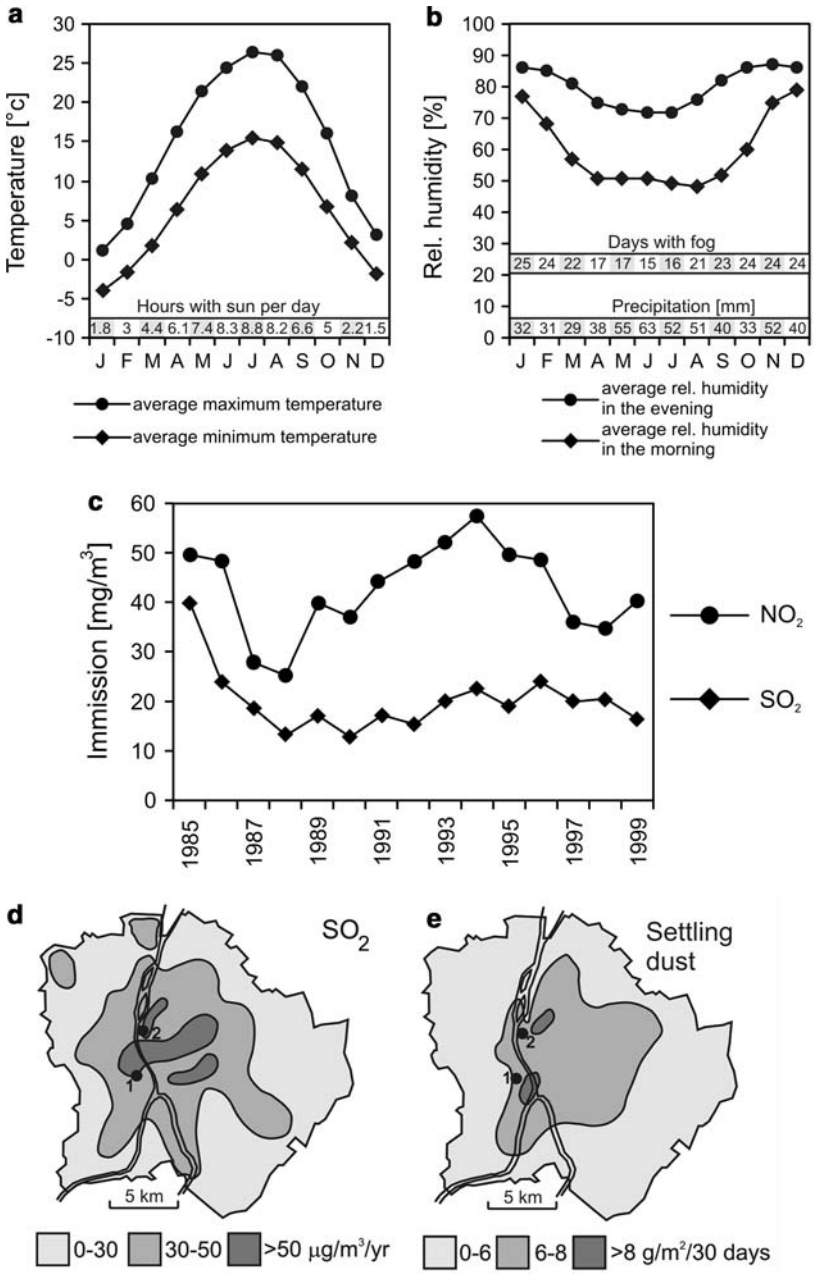

Fig. 1 Climate and pollution data of Budapest; **a** annual monthly average temperature and sunny days, **b** relative humidity, monthly precipitation and foggy days, **c** NO_2 and SO_2 trends; **d** map of Budapest with the distribution of SO_2 (1 Citadella, 2 Parliament House). **e** Map of Budapest with the distribution of settling dust (1 Citadella, 2 Parliament House). Data sources: **a–c** Hungarian Meteorological Institute, **d** and **e** Török (2002)

in Budapest. In historic buildings, the footings, window cornices and exposed ornaments were made from this lithotype in the past (Török 2006a). Nowadays, travertine is particularly applied as a replacement stone in reconstruction works. A prominent example is the Parliament building where the miocene limestone has been replaced with travertine (Hüpers et al. 2005). Travertine quarries are found in the north of Budapest (Süttõ). The unweathered freshwater limestone has a creamy whitish colour and is mainly composed of fine-grained calcite (<0.1 mm). Accessory minerals are quartz and muscovite. The porosity is generally very low and is mainly developed as interparticle pores and dissolutional vugs.

Methods

To understand the influence of rain/wind exposure in the formation process of weathering forms and stone decay, two walls were mapped at the Citadella. One wall is exposed to prevailing winds and faces NNE, whereas the other wall is sheltered from direct rain-wash and faces SSW. The visual assessment and

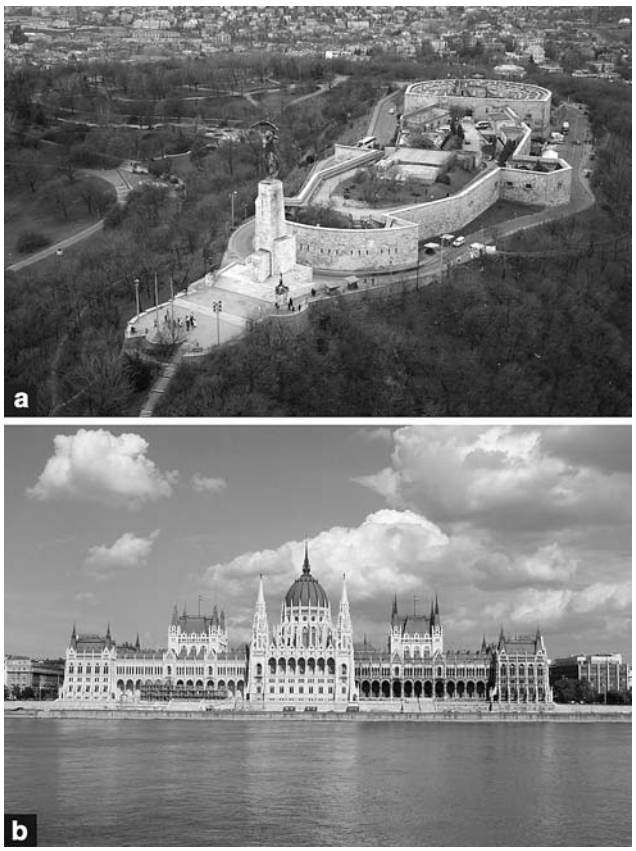

Fig. 2 Distant view of the Citadella (**a**) and the Parliament building (**b**) in Budapest (**a** is from the Hungarian Press Institute)

description of the weathering features were made using the methodology of Fitzner and Heinrichs (2002). Damage categories were also calculated according to Fitzner and Heinrichs (2002) for each stone block, considering the depth of weathering and the proportion of the back-weathered surface area. Seven damage categories were defined, showing a successive increase in loss of stone material from the lowest (no damage) to the highest damage category.

At other localities, sampling of selected crusts from miocene limestone and Pliocene freshwater limestone for mineralogical and geochemical analyses were performed. Crust samples (28) were collected from the coarse-grained miocene limestone at the Citadella fortress. An additional 14 samples of the miocene limestone (coarse- to fine-grained) and pliocene freshwater limestone were collected from the Parliament building as well as from eight alternate locations in the centre of Budapest.

The presented chemical data focuses on major elements (C, Ca, Si, S) and heavy metals (Ti, Al, Fe, Mn, Zn) of the host rocks and crusts. The chemical composition was obtained by X-ray fluorescence spectroscopy using a Phillips PW1480. The detection error for major elements is <1% and for trace elements 5–10%. Sulphur and carbon were additionally analysed by means of an automatic analyser METALYT CS 1000RF (Eltra Gmbh) with an error of 5%. The mineralogical composition was determined by X-ray diffraction (XRD) using a Phillips PW1800 Diffractometer. Microfabric studies were done on samples impregnated with blue epoxi-resin to visualize the pore system and with scanning electron microscopy (LEO 1455 Gemini).

To determine the sources of sulphur, 18 samples from different locations were measured for sulphur isotopes. These samples were black and white crusts collected from the coarse-grained limestone and black crusts from the freshwater limestone. The sulphur in the samples was freed as SO_2 by heating up to 900°C together with Vanadinpentoxid and measured by a FINNIGAN Gasspectrometer DELTA VE. For detailed sample preparation, see Klemm and Siedel (1999). To identify the possible sources, rainwater was collected and SO_2 from air was sampled with K_2CO_3 saturated filter papers. The value of $\delta^{32}S$ for rainwater was 6.1‰. SO_2 determination failed due to sparse sulphur accumulation on the filter papers. A possible cause could be the dilution of K_2CO_3, which originated from wetting of the filter papers.

Decay features and their extent

A great variety of decay features are found in oolitic limestones. The most frequent weathering forms are the crusts showing variations in colour, morphology and thickness (Török and Rozgonyi 2004). Surface loss is commonly observed as back weathering and crust detachment, which is followed by granular disintegration. Thin weathering crusts tend to show flakes and scales. Deposition of airborne particulates, surface discolouration and soiling are also commonly observed.

The commonest weathering forms at the Citadella were the white crusts. These usually cover the whole surface of ashlars and occur as cemented layers at the stone surface. According to their thickness (1) thin and (2) thick white crusts were identified.

Thick white crusts have a thickness of a few millimetres to up to 2 cm and are mostly found on rain or wind exposed surfaces (Fig. 4a). The crust surface is generally smooth, well cemented and practically impermeable (Török 2002). This is caused by recrystallization processes, leading to a complete occlusion of pores. Thus, thick case-hardened white crusts are formed composing of a well-cemented upper zone

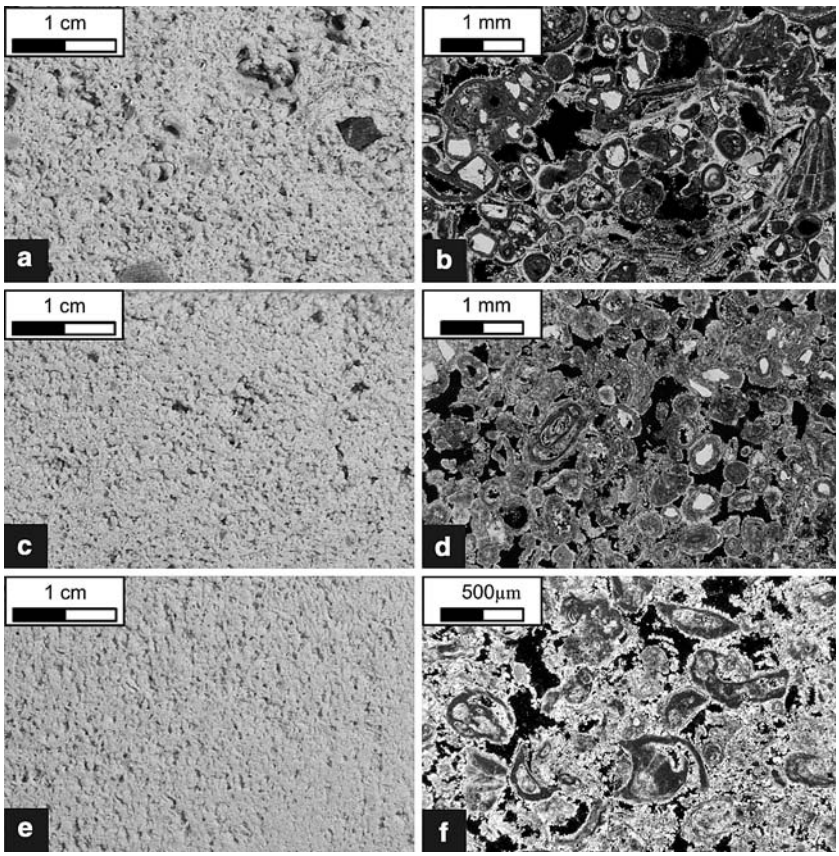

Fig. 3 Limestone types and their microfabrics: coarse oolitic limestone with quartz particles and lithic clasts (**a**) and its bioclastic micro-oncoidal grainstone microfacies (**b**), medium-grained oolitic limestone (**c**) with well- rounded micro-oncoids and foraminifers (**d**), fine-grained limestone (**e**) with miliolid forams and microsparitic cement (**f**)

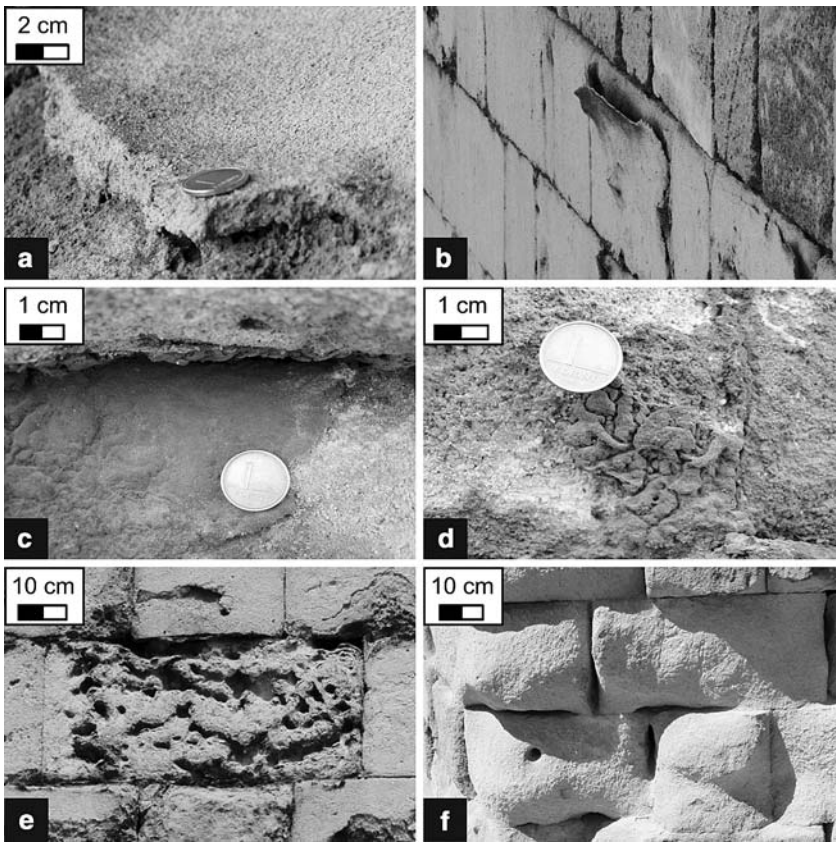

Fig. 4 Decay forms of oolitic limestone: **a** thick scaling white crust, **b** contour scaling white crust, **c** laminar black crust (central part of the picture), **d** framboidal black crust, **e** hollowing and black crust formation in surface depressions, **f** rapid surface loss due to granular disintegration

(decrease in surface porosity) and a softer underside (Török et al. 2006). Contour scaling is often linked to thick case-hardened white crusts (Fig. 4b). After scaling of the crust, granular disintegration begins leading to rapid and catastrophic surface loss.

Thin white crusts are never thicker than 1 mm. They have a relatively smooth outer surface and are typical features of both well-exposed and partly sheltered ashlars. Typical detachment mechanisms such as scaling, blistering and multiple flaking frequently occur on poorly cemented thin white crusts. Mechanical breakdown of these crusts due to weathering depends on the rate of cementation, the adherence to the stone surface and mineralogy.

The growth of black crusts is usually confined to moderately exposed or sheltered wall sections providing some shelter against wind and from direct rainwash. According to their morphology, black crusts are divided into (1) thin laminar crusts and (2) framboidal black crusts.

Thin laminar crusts often follow the stone surfaces and are found on vertical or sub-vertical walls. These black crusts are only a few millimetres thick and their surfaces are very smooth (Fig. 4c). When there is a particular shelter and a moist area, the laminar black crusts can transform to their framboidal counterparts. Blistering and scaling are common breakdown features of these crusts, but in general they form a rigid and hard cover on the oolitic limestone.

The framboidal black crusts (also called globular black crusts or dendritic black crusts) appear in the form of small globules or spherules that can reach a thickness of a few centimetres (Fig. 4d). In general, these crusts grow on protected parts of walls such as joints between ashlars or sheltered interiors of bullet holes caused by war damage. Blistering or the removal of the entire crust by scaling is the breakdown feature of these crusts.

Besides crust removal, the surface loss is also attributed to rare alveolar weathering (Fig. 4e) and granular disintegration (Fig. 4f). When no secondary crust is formed, the backstepping of the surface due to granular disintegration can be in the order of 5–10 cm (Fig. 4f).

The percentages of surface cover of weathering features on sheltered and exposed walls are different (Fig. 5a). The most frequent weathering features on both walls are the white crusts (Fig. 5b). The appraisal of stone damage by means of damage categories indicates that most of the ashlars on the Citadella are affected by moderate damage (Fig. 5c). Damage categories calculated for rows of ashlars indicate that severe stone damage especially occurs in the lower

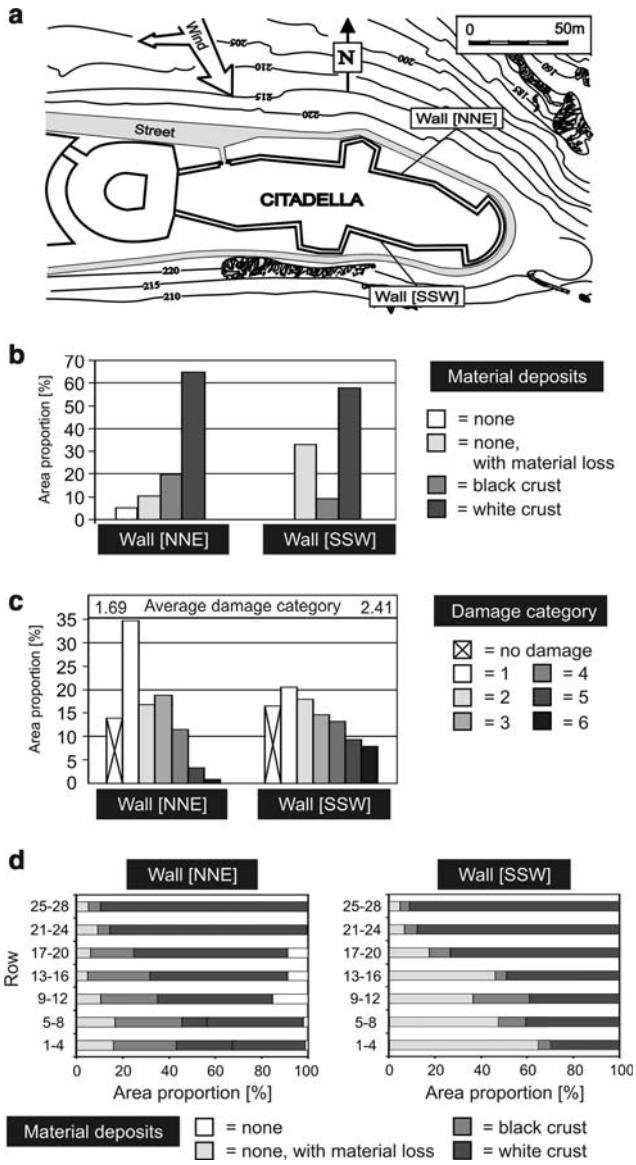

Fig. 5 The Citadella and the frequency of weathering forms and damage categories: **a** site map showing the location of mapped walls, **b** percentage of weathering crusts and material loss, **c** damage categories and **d** percentage of weathering crusts and material loss in rows of ashlars

parts of the walls. Furthermore, the damage also depends on the exposure of the wall. The exposed NNE wall is less damaged (average damage category of 1.69 out of 6) than the rain/wind-sheltered SSW wall, which shows a more severe loss of stone material with an average damage category of 2.41 out of 6 (Fig. 5c). Considerable amounts of badly damaged ashlars (damage categories 5 and 6) are found especially on the SSW (sheltered) wall.

The analysis of crusts and material loss considering the rows of ashlars show that there is a bottom-up increase in white crusts (Fig. 5d). An opposite trend of

stone material loss and back weathering was recorded, i.e. the low-lying rows display more severe material loss in the form of granular disintegration.

In contrast to white crusts, black crusts frequently occur on wall sections with some shelter against wind and from rain-wash. Thus, such a vertical distribution shown by white crusts is not clearly documented for black crusts (Fig. 5d).

Mineralogy, fabric and geochemistry of the crusts

Host rock

Unweathered samples were taken from deeper parts of slightly weathered host rocks to characterize the mineralogical and geochemical changes due to the weathering. Fresh samples were also collected from Sóskút quarry, 30 km SE of Budapest. The quarry samples are dominated by high calcium and carbon contents with lower values for the coarse-grained varieties (34.36 wt% Ca, 10.70 wt% C) and slightly higher concentrations for the fine-grained ones (38.93 wt% Ca, 11.98 wt% C). The higher silicon content of the coarse-grained limestone (4.58 wt% Si) concurs well with macroscopically observed quartz and feldspar particles, while the fine-grained limestone is less silicon-rich (0.75 wt%). The values for elements such as Fe, Al, Ti, Mn and S are below 0.5 wt%. The concentration of zinc is below 10 ppm. The average geochemical composition of the freshwater limestone is comparable to the fine-grained limestone (cf. Table 1).

White crusts

White crusts can be observed exclusively on the porous miocene limestones. In cross sections of the white crusts, both solution and precipitation phenomena occur. Solution features are especially noticeable along the crystal surfaces and cleavage planes of calcite. The solution and re-precipitation of calcite lead to strengthening of the surface area. This is clearly documented by a decrease in the pore space and an increase in microsparitic and micritic cement near the stone surface in the crust (Fig. 6a). Concurrently, dissolution may cause a differential back weathering and microkarst features at the surface of some ashlars. Additionally, the medium- and coarse-grained limestones can display a beginning of crust detachment along newly formed cracks. The cracks are mainly parallel to the surface with an average width of 0.5 mm and a length of 10 mm. Along wider opened cracks, typical idiomorphic gypsum crystals of dark colour can be recognized under the SEM (Fig. 6b).

Thin and thick white crusts show the same range of element concentrations, characterized by high calcium, carbon and silicon contents (Table 1). Compared to the unaltered host rocks, white crusts have slightly lower values for calcium, carbon, aluminium and iron. The major components of the middle-grained limestone show the same trend, while the average values for iron and aluminium are a little bit higher for thick white crusts. However, the most obvious difference is the presence of sulphur in white crusts with concentrations ranging from 0.5 to 5.6 wt%. Zinc is also enriched in thin

Table 1 Geochemical data of various crust types and host rock (average data of *n* analyses)

		C (tot) (%)	S (%)	Si (%)	Ti (%)	Al (%)	Fe (tot) (%)	Mn (%)	Mg (%)	Ca (%)	Zn (ppm)
Host rock											
Coarse grained limestone	$n = 1$	10.70	0.06	4.58	0.03	0.23	0.13	0.01	0.48	34.36	6.00
Middle grained limestone	$n = 1$	10.78	0.06	5.05	0.04	0.23	0.12	0.01	0.48	34.53	5.00
Fine grained limestone	$n = 1$	11.98	0.04	0.75	0.02	0.11	0.09	0.01	0.42	38.93	8.00
Freshwater limestone	$n = 1$	11.92	0.11	0.93	0.02	0.14	0.08	0.01	0.37	38.76	6.00
Thin White crust											
Coarse grained limestone	$n = 7$	7.70	5.52	3.33	0.03	0.19	0.11	0.01	0.36	28.96	221.86
Thick White crust											
Coarse grained limestone	$n = 5$	8.51	3.70	3.39	0.03	0.20	0.11	0.01	0.37	28.69	32.20
Middle grained limestone	$n = 2$	9.69	1.68	4.88	0.04	0.27	0.16	0.01	0.43	32.34	24.50
Thin black crust											
Coarse grained limestone	$n = 5$	6.02	7.11	3.93	0.04	0.32	0.21	0.01	0.41	23.95	69.60
Middle grained limestone	$n = 1$	8.15	4.35	4.86	0.04	0.31	0.21	0.01	0.37	28.62	44.00
Fine grained limestone	$n = 1$	9.57	3.14	0.14	0.01	0.06	0.08	0.01	0.43	34.53	28.00
Freshwater limestone	$n = 1$	9.03	3.24	1.68	0.03	0.14	0.10	0.00	0.43	32.73	55.00
Thick lack crust											
Coarse grained limestone	$n = 14$	3.52	10.87	3.98	0.05	0.42	0.28	0.01	0.42	19.26	165.50
Freshwater limestone	$n = 9$	2.95	12.20	4.47	0.07	0.48	0.32	0.01	0.30	18.80	89.56

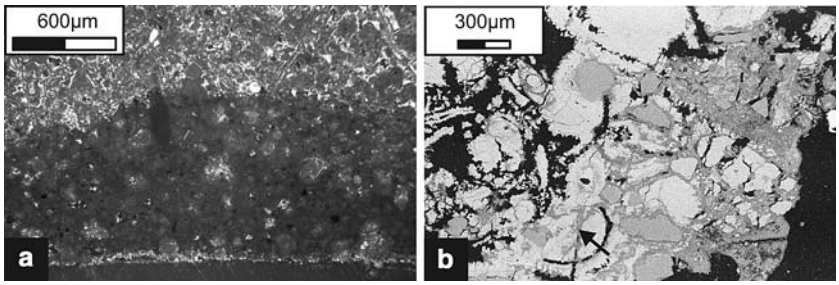

Fig. 6 Microscopic images of white crust: **a** cemented microsparitic to micritic calcite forms a thin zone at the stone surface (dark zone at the bottom part) and **b** BSEM image of cemented white crust with small gypsum crystals partly healing micro-cracks (*arrow*)

white crusts with average values of 222 ppm. To characterize the element mobility during weathering, i.e. enrichment or depletion, enrichment factors (EF) were calculated with reference to titanium as an indicator element (Sabbioni 2003). For thin and thick white crusts, enrichment factors are close to 1 for C, Ca, Si and Al. These ratios indicate that these crusts are geochemically more or less comparable to the host rocks and fit also with the microscopically observed solution/precipitation of calcite. In comparison with typical Si/Al-, Fe/Al- and Al/Ti- ratios of aerosols, crusts collected from the coarse-grained limestone show high ratios close to the reference (Table 2). Nevertheless, elements like S, Zn and Mn are enriched in white crusts and refer therefore to an atmospheric source.

Black crusts

Microscopic observations reveal that black crusts (Fig. 7) are dominated by gypsum. Thick crusts of freshwater limestone are characterized by a layer of acicular gypsum crystals oriented perpendicularly to the surface of the host rock. Above this layer, the gypsum forms sparse crystals and crystal aggregates. Additionally, quartz and feldspar particles (<0.1 mm) are visible. Evenly spread opaque particles are identified as organic particles. The brownish colour can also be originated from iron-oxides (Do 2000). Accordingly, thin and thick black crusts of the miocene limestone are ascribed as mixture layers of gypsum, organic compounds, iron-oxides, quartz and feldspar particles and calcite (<0.5 mm). Compared to the white crusts, the micro-cracks are particularly well developed. These cracks ultimately propagate and finally lead to the detachment of the crusts. When cracks are very common and the surface is in an advanced stage of cracking, flaking of the crust is observed. The width of these detached zones can be up to 0.2–0.3 mm. The flaking does not solely occur at the crust/host rock interface. It may also be traced at depth within the uppermost layer of the host rock, just below the crust. On the other hand, intact layers of thin crusts can also provide a temporary protection of the host rock due to gypsum-healed cracks near or within the stone surface.

Table 2 Si/Al, Fe/Al and Al/Ti ratios of aerosol (after Rahn 1976 and Steiger 1991), host limestone and weathering crusts

	Si/Al	Fe/Al	Al/Ti
Aerosol	2.7	1–3	10–15
Coarse-grained limestone	20.1449	0.5536	6.7743
Thin white crust	21.0768	0.6274	6.8129
Thick white crust	18.9115	0.5910	7.0003
Thin black crust	11.2798	0.6608	8.1376
Thick black crust	9.5942	0.6135	8.4563

The mineralogical composition is characterized by high gypsum content, together with calcite, quartz and feldspar. The average sulphur content is between 3.14 and 7.11 wt% for thin black crusts and thick black crusts have average values of 10.87 and 12.20 wt%. On the other hand, an apparent loss of calcium (most

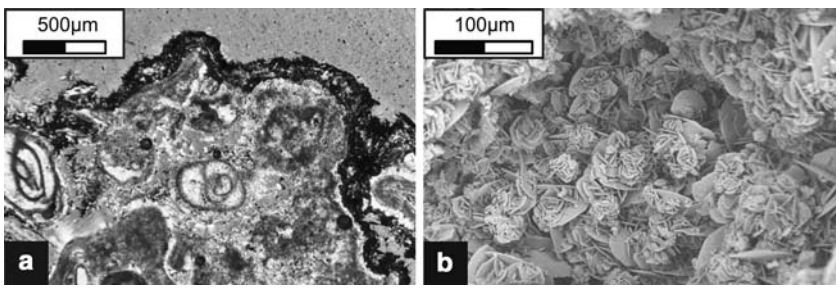

Fig. 7 Black crusts under microscope: **a** thin-section photograph of a thin black crust composed of dark coloured organic and opaque particles, small gypsum crystals, calcite micrite, quartz and feldspar particles and **b** SEM image of gypsum rosettes on the surface of the black crust

prominently in thick black crusts) and carbon (also in thick black crusts) can be recognized (Table 1). In addition, the proportion of heavy metals is also significantly increased for titanium, aluminium, iron and zinc. The fine-grained limestone is an exception to the described trends. Only zinc is considerably increased in thin black crusts, while titanium, aluminium and iron have lower values. Calculated enrichment factors for major elements like Ca, C and Mn in the black crusts are depleted, whereas metals like Fe and Al are slightly enriched. The highest enrichment factor for black crust was observed for sulphur (Fig. 8).

Discussion

Mapping of oolitic limestone ashlars have revealed that weathering crusts are the most common weathering features in the city of Budapest. Both white and black crusts were identified with various proportions on exposed and sheltered walls. The most frequent crusts are white crusts that are mostly formed in wind/rain-exposed parts of façades, but also common on sheltered walls (Fig. 5b). This observation is not in accordance with most previous works (Amoroso and Fassina 1983; Marvelaki-Kalaitzaki and Biscontin 1999), where white areas were only associated with exposed areas. One possible explanation is the presence of moisture, high acidity and high concentration of air pollutants, which allow the formation of an impermeable crust on vertical surfaces not exposed to direct rain-wash. This study has also documented that black crusts and white crusts are more common on wind/rain-exposed parts than on sheltered walls (Fig. 5b). One would expect a different trend: more frequent black crusts on sheltered parts and more abundant white crusts on exposed walls. Thus, we can assume that crust formation is governed by wind-driven particulates and atmospheric pollutants (Sabbioni 1995; Primerano et al. 2000) and is more intense on exposed façades. It is also important to note that the walls, where crusts are more common, show less deterioration than the sheltered walls where crusts are less frequent. In other words, the sheltered wall has an average damage category of 2.41, while the calculated average damage category is 1.69 for the exposed and crust covered wall (Fig. 5c). These numbers suggest that crust formation can slow down surface retreat and might stabilize the stone surface. It is in accordance with the observations of Török (2002, 2003) and Török et al. (2006) who emphasized the protective role of weathering crusts on oolitic limestones. Secondary and tertiary crusts (Smith et al. 2003) can also develop and provide further stabilization and a decline in surface retreat. The mechanism of slowing down material loss, short-term stability, which is followed by rapid decay, has been thoroughly discussed by Smith (1996).

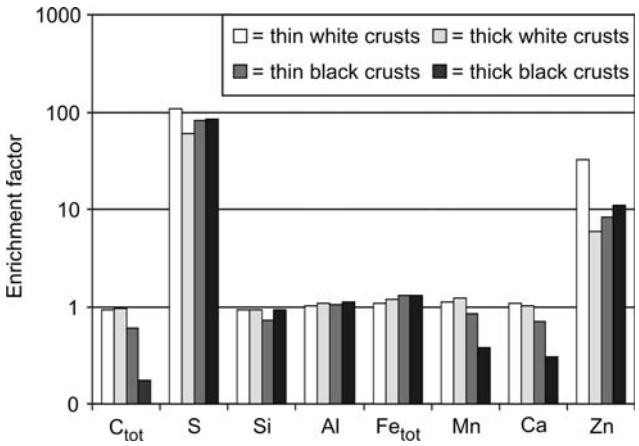

Fig. 8 Average calculated enrichment factors of thin and thick white and black crusts (see text for further explanation)

Stone material loss and back weathering are preferentially found in low-lying rows, mostly in the form of granular disintegration (Fig. 4f). Thus, intense weathering-related surface loss is commonly associated with ashlars from which crusts have already been detached. Hence, a faster weathering process takes place in the lower parts of the studied walls. In contrast to white crusts, black crusts frequently occur on wall sections providing some shelter against direct rain-wash. The percentage of black crusts covered areas slightly decreases from the ground level upward in exposed walls (Fig. 5d). The proportion of white crusts covered areas shows a gradual increase from the ground level upward both on sheltered and exposed walls (Fig. 5d), indicating that microclimatic conditions and moisture availability are key factors in crust formation. Further evidence supporting this theory is the fact that at about 5–6 m above ground level, no significant difference between the proportions of black/white crusts were recorded in the exposed and sheltered walls (Fig. 5d).

The mechanism of black crust formation has been investigated thoroughly under simulated laboratory conditions (Rodriguez-Navarro and Sebastian 1996; Ausset et al. 1999; Cultrone et al. 2004) and in the field (Amoroso and Fassina 1983; Winkler 1970; Sabbioni 1995; Moropoulou et al. 1998; Antill and Viles 1999; Fassina et al. 2002; Török and Rozgonyi 2004; Bonazza et al. 2005; Török 2006a). However, there are no previous papers dealing with white crust formation under laboratory conditions, although white crusts are more

commonly found on limestone buildings than black crusts.

Two types of white crusts, thin and thick ones, were identified on oolitic limestone ashlars in Budapest (Török 2002, 2003; Hüpers et al. 2005; Török et al. 2006) (Figs. 4, 6). The formation mechanism of both types is similar. Microscopic studies revealed that white crusts consist of cemented zones that are found on the surface of the ashlars (Fig. 6a). In these zones, the pores are occluded either by microcrystalline calcite (Fig. 6a) or gypsum (Fig. 6b). It has been also confirmed that white crusts are less porous than the host rock (Török 2003; Török et al. 2006). Consequently, it is supposed that surface dissolution and reprecipitation of calcite lead to the formation of mainly calcite-cemented crust. Gypsum is an accessory mineral, which can have a contribution to the crust of up to 70%, but more often to 45% (Török and Rozgonyi 2004). Besides petrographic analyses (Fig. 6b), our XRF analyses also confirmed the presence of sulphur and thus gypsum in white crusts (Table 1). Hüpers et al. (2005) and Török et al. (2006) have demonstrated that crust formation on oolitic limestones leads to a porosity loss of 4–6% in the crust zone. Experiments with Karsten tube have also shown that white crust forms an impermeable layer at the stone surface (Török 2003).

In accordance with previous studies (Török 2002, 2003, 2005; Hüpers et al. 2005) two different kinds of black crusts were identified both on porous limestone and on freshwater limestone: thin laminar black crusts and framboidal thick black crusts. Both crusts types develop in areas that are sheltered from direct rainwash. Microscopically two different textures of framboidal black crusts were identified (Fig. 7) depending on the microfabric of the substrate. On freshwater limestone, a layer of gypsum crystals along the contact line of the host rock and crust was observed, while on coarse limestone this lowest layer is characterized by gypsum, calcite and quartz.

For the crust formation, moisture is needed (Amoroso and Fassina 1983). Considering the climatic conditions, the high relative humidity, common fogs (cf. Del Monte and Rossi 1997) and dew, in Budapest, ensure moisture for crust formation (Fig. 2). Dissolution in the sheltered wall is not as intense as on rainwashed exposed areas, where white crusts and not their black counterparts are found. Hence, it is suggested that evaporation leads to the precipitation of gypsum. Besides gypsum, quartz, organic particles were also found. Smith et al (2003) have also proved that airborne dust in Budapest consists of silt-sized debris, carbonaceous and siliceous particles and organic debris. The contribution of particulates to the formation of black crusts have been already confirmed in many urban areas throughout Europe (Bonazza et al. 2005), including Athens (Moropoulou et al. 1998), Bologna (Del Monte et al. 2001), London (Trudgill et al. 2001), Milan (Bonazza et al. 2004), Oxford (Viles 1994; Thornbush and Viles 2004), Paris (Lefèvre and Ausset 2002) and Venice (Amoroso and Fassina 1983; Del Monte and Vittori 1985; Smith et al. 1988; Fassina et al. 2002). The highest sulphur content in weathering crusts of Budapest was measured in thick black crusts, which show framboidal morphology (Table 1; Fig. 4d). It is in accordance with the previous observations (Török 2002, 2005) and confirms that framboidal morphology provides larger reaction surface and enables fog and dew derived moisture condensation. Thus, more water is available at the surface of framboidal crust than at laminar crust formation and gypsum precipitation is faster. Dust particles and organic carbon play an important role in black crust formation in Budapest (Smith et al. 2003; Török 2006b) by providing nucleation sites for gypsum crystal growth. Laboratory simulations also confirmed the catalytic role of organic carbon in the formation of gypsum (Rodriguez-Navarro and Sebastian 1996; Ausset et al. 1999).

The chemical compositions of white and black crusts are characterized by one common feature: a uniform enrichment in the sulphur content (Table 1), with enrichment factors of 50–100 (Fig. 8). The most important sulphur sources are SO_2-deposition from air and SO_4^{2-} from rainwater (Neumann et al. 1993). Due to the lack of $\delta^{32}S$ values for SO_2 in Budapest, it is not possible to distinguish between the two mentioned sources. Nevertheless, the $\delta^{32}S$ value for rain is close to the measured range for the crusts and thus it can be suggested that SO_4^{2-} from rainwater is involved in the formation of gypsum (Fig. 9). Analysing isotopic composition of black crusts of monuments in Antwerp, Torfs et al. (1997) found that gypsum is primarily related to SO_2 and less probably to SO_4^{2-}. In the city of Dresden, weathering crusts on historical buildings were found to have a sulphur isotopic composition of +5.7 and +10.1, while the isotope ratios in rainwater were slightly less enriched in heavy sulphur, +4.4 and +7.7, but still higher than that of the atmospheric SO_2, +0.3 and +4.5 (Klemm and Siedel 2002).

The sulphur isotopic compositions of white and black crusts overlap (Fig. 9), which points to an identical sulphur source. It is independent of the exposure conditions of the buildings, and crusts are more enriched with heavy sulphur isotopes compared to rainwater, which trend was also observed in Dresden

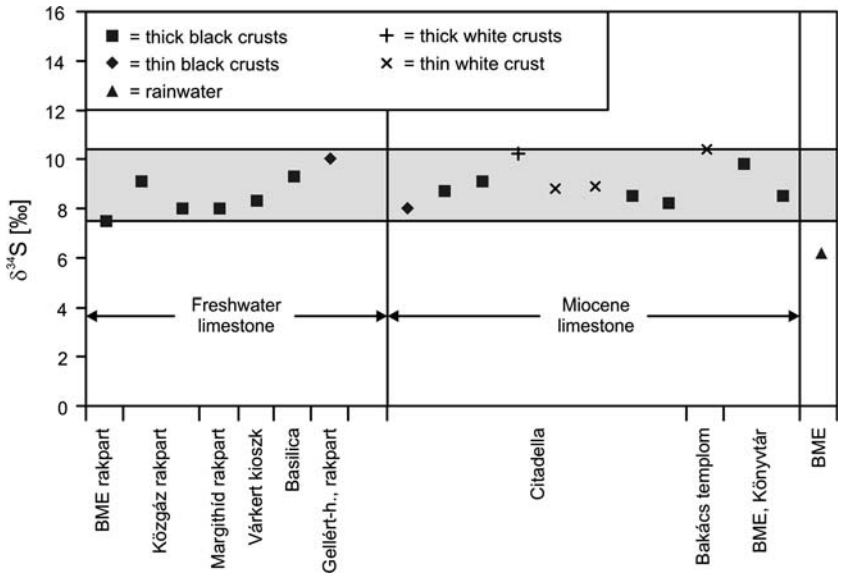

Fig. 9 Stable sulphur isotopic composition of black and white crusts with reference to rainwater composition

(Klemm and Siedel 2002). The slightly heavier sulphur in the crusts compared to the sulphate in the rainwater is most probably derived from dust particles. This observation is strongly supported by the mineralogical and chemical composition of the crust, especially the black ones. Laboratory analyses of sulphate rich fog water confirmed that 60 h after a main fog event, gypsum crystals were formed (Del Monte and Rossi 1997). Hence, we suggest that the sulphur in the gypsum-rich black crusts of Budapest is derived from similar sources but, due to climatic conditions (Fig. 2), probably SO_4^{2-} rich rainwaters and fogs have increased importance compared to SO_2.

Chemical investigations revealed that alongside sulphur, Zn is also highly enriched in the crusts (Fig. 8). The presence of Zn is due to an intense impact of combustion emissions (steel and chemical industry). Zn mostly accumulates in the street dust of Budapest and is bound by the exchangeable/carbonate phase (McAlister et al. 2006).

The Si/Al ratio of thick black crusts is the lowest, while the Al/Ti ratio is the highest and the closest to aerosol (Table 2) indicating a contribution of airborne particulates to black crust formation.

Biological activity may also contribute to black crust formation (Krumbein 1992). However, biological activity is significantly reduced in polluted urban environments (Warscheid and Braams 2000) like that of Budapest and thus its contribution to black crust formation is limited (Hüpers et al. 2005; Török et al. 2006). Saiz-Jimenez (1993, 1995) also pointed out that it is possible to make a difference between biogenic carbon and pollution related carbon sources.

Accordingly, black crust formation is related to air pollution, both particulate (dust) and liquid and gaseous sources. A complex process of dissolution and re-precipitation takes place at the stone/air interface leading to the formation of black crust.

Conclusion

Air pollution in Budapest leads to accelerated weathering of limestones. Weathering crusts are the most common decay features, with two types of white and two types of black varieties. The mineralogical composition of crusts is less influenced by the host rock lithology, but mostly depends on the crust morphology.

Organic carbon-rich dust serves as a catalyst and accelerates gypsum precipitation on black crust covered areas. White crusts also contain gypsum, but the proportion of calcite is higher than that of the gypsum. Solution and recrystallization of calcite, as well as deposition of airborne particles and air pollutants, are the primary processes acting on white crusts.

The high sulphur concentration in Budapest, the continental climate and frequent fogs enable the formation of sulphur-rich layers on limestone surfaces due to condensation.

Chemical analyses underlie the role of airborne particles in crust formation. The crusts are enriched with sulphur and have a slightly elevated sulphur isotope ratio compared to the adjacent rainwater. The higher reaction surface of framboidal black crusts alongside the wind-driven particulates leads to accumulation of gypsum crusts.

The geochemical compositions of black and white crusts show some differences and even enable the marking of differences in the microfabric of the host rock.

Exposed and non-exposed walls show differences in percentage of weathering features and damages. Surprisingly, black crusts are also quite common on exposed walls, but this is probably due to high pollution levels. The crusts are more common on exposed walls than on sheltered ones, but sheltered walls show a higher loss of stone material (higher damage categories) due to loss of crusts.

Acknowledgments The financial support of the German-Hungarian Scientific co-operation (DAAD-MÖB project no. 30) is acknowledged. This work was also partly financed by the Bolyai János research grant (BO/233/04, ÁT) and by the Hungarian Science Found (OTKA, grant no. K63399, ÁT).

References

Amoroso GG, Fassina V (1983) Stone decay and conservation. Elsevier, Amsterdam, pp 1–453

Antill SJ, Viles HA (1999) Deciphering the impacts of traffic on stone decay in Oxford: some preliminary observations from old limestone walls. In: Jones MS, Wakefield RD (eds) Aspects of stone weathering, decay and conservation. Imperial College Press, London, pp 28–42

Ausset P, Del Monte M, Lèfevre RA (1999) Embryonic sulphated black crusts on carbonate rocks in atmospheric simulation chamber and in the field: role of carbonaceous fly-ash. Atmos Environ 33:1525–1534

Bonazza A, Sabbioni C, Ghedini N, Favoni O, Zappia G (2004) Carbon data in black crusts on European monuments. In: Saiz-Jimenez C (ed) Air pollution and cultural heritage. Taylor & Francis, London, pp 39–47

Bonazza A, Sabbioni C, Ghedini N (2005) Quantitative data on carbon fractions in interpretation of black crusts and soiling on European built heritage. Atmos Environ 39:2607–2618

Cultrone G, Rodriguez-Navarro C, Sebastian E (2004) Limestone and brick decay in simulated polluted atmosphere: the role of particulate matter. In: Saiz-Jimenez C (ed) Air pollution and Cultural Heritage. Taylor & Francis, London, pp 141–145

Del Monte M, Rossi P (1997) Fog and gypsum crystals on building materials. Atmos Environ 31:1637–1646

Del Monte M, Vittori O (1985) Air pollution and stone decay: the case of Venice. Endeavoir 9:117–122

Del Monte M, Ausset P, Forti P, Lefèvre RA, Tolomelli M (2001) Air pollution records on selenite in the urban environment. Atmos Environ 35:3885–3896

Do J (2000) Untersuchung der Verwitterung von Fassaden aus Naturstein—Vergleich an den Gebäuden der Museumsinsel in Berlin. Ph.D. University of Berlin

Fassina V, Favaro M, Naccari A (2002) Principal decay patterns on Venetian Monuments. In: Siegesmund S, Weiss T, Vollbrecht A (eds) Natural stones, weathering phenomena, conservation strategies and case studies. Geological Society, London Special Publication 205:381–391

Fitzner B, Heinrichs K (2002) Damage diagnosis at stone monuments—weathering forms, damage categories and damage indices. In: Prykril R, Viles (eds) Understanding and managing stone decay. Carolinum Press, Prague, pp 11–56

Hüpers A, Müller C, Siegesmund S, Hoppert M, Weiss T, Török Á (2005) Kalksteinverwitterung—die Zitadella und das Parlamentsgebäude in Budapest. In: Siegesmund S, Auras M, Snethlage R (eds) Stein Zerfall und Konservierung. Edition Leipzig, Leipzig, pp 201–209

Kieslinger A (1932) Zerstörung an Steinbauten—Ihre Ursachen und ihre Abwehr. Verlag Deuticke, Leipzig-Wien, pp 1–346

Klemm W, Siedel H (1999) Schwefelisotopenanalyse von bauschädlichen Sulfatsalzen an historischen Bauwerken. Wissenschaftliche Mitt 8/99:1–101

Klemm W, Siedel H (2002) Evaluation of the origin of sulphate compounds in building stone by sulphur isotope ratio. In: Siegesmund S, Weiss T, Vollbrecht A (eds) Natural stones, weathering phenomena, conservation strategies and case studies. Geological Society, London Special Publication 205:419–429

Krumbein, WE (1992) Colour changes of building stones and their direct and indirect biological causes. In: Rodriguez JD, Henriquez F, Jeremias FT (eds) Seventh international congress on deterioration and conservation of stone, Lisbon, pp 443–452

Lefèvre RA, Ausset P (2002) Atmospheric pollution and building materials: stone and glass. In: Siegesmund S, Weiss T, Vollbrecht A (eds) Natural stones, weathering phenomena, conservation strategies and case studies. Geological Society, London Special Publication 205:329–345

McAlister JJ, Smith BJ, Török Á (2006) Element partitioning and potential mobility within surface dusts on buildings in a polluted urban environment, Budapest. Atmos Environ (in press)

Maravelaki-Kalaitzaki P, Biscontin G (1999) Origin, characteristics and morphology of weathering crusts on Istria stone in Venice. Atmos Environ 33:1699–1709

Moropoulou A, Bisbikou K, Torfs K, Van Grieken R, Zezza F, Macri F (1998) Origin and growth of weathering crusts on ancient marbles in industrial atmosphere. Atmos Environ 32:967–982

Neumann HH, Steiger M, Wassmann A, Dannecker W (1993) Aufbau und Ausbildung schwarzer Gipskrusten und damit zusammenhängender Gefügeschäden von Naturwerksteinen am Beispiel des Leineschlosses (Hannover). Jahresber Steinzerfall Steinkonservierung 1991:150–167

Sabbioni C (1995) Contribution of atmospheric deposition to the formation of damage layers. Sci Total Environ 167:49–56

Sabbioni C (2003) Mechanism of air pollution damage to stone. In: Brimblecombe P (ed): The Effects of air pollution on the built environment. Air Pollut Rev 2:63–88

Primerano P, Marino G, Di Pasquale S, Mavilia L, Corigliano F (2000) Possible alteration of monuments caused by particles emitted into the atmosphere carrying strong primary acidity. Atmos Environ 34:3889–3896

Rhan KA (1976) Silicon and aluminium in atmospheric aerosols: crust–air fractionation. Atmos Environ 10:597–601

Rodriguez-Navarro C, Sebastian E (1996) Role of particulate matter from vehicle exhaust on porous building stones (limestone) sulfation. Sci Total Environ 187: 79–91

Saiz-Jimenez C (1993) Deposition of airborne organic pollutants on historic buildings. Atmos Environ 27B:77–85

Saiz-Jimenez C (1995) Microbial melanins in stone monuments. Sci Total Environ 167:273–286

Smith BJ (1996) Scale problems in interpretation of urban stone decay. In: Smith BJ, Warke PA (eds) Processes of urban stone decay. Donhead, London, pp 3–18

Smith BJ, Whalley WB, Fassina V (1988) Elusive solution to monumental stone decay. New Sci 1615:49–53

Smith BJ, Török Á, McAlister JJ, Megarry J (2003) Observations on the factors influencing stability of building stones following contour scaling: a case study of the oolitic limestones from Budapest, Hungary. Build Environ 38:1173–1183

Steiger M (1991) Die anthropogenen und natürlichen Quellen urbaner und mariner Aerosole, charakterisiert und quantifiziert durch Multielementanalyse und chemische Receptormodelle. Ph.D. University of Hamburg, Hamburg

Thornbush M, Viles H (2004) Integrated digital photography and image processing for the quantification of colouration on soiled limestone surfaces in Oxford, England. J Cult Herit 5:285–290

Torfs KM, Van Grieken RE (1997) Chemical relations between atmospheric aerosols, deposition and stone decay layers on historic buildings at the Mediterranean coast. Atmos Environ 31:2179–2192

Trudgill ST, Viles HA, Inkpen R, Moses C, Gosling W, Yates T, Collier P, Smith DI, Cooke RU (2001) Twenty-year weathering remeasurements at St Paul's Cathedral, London. Earth Surf Processes Landf 26:1129–1142

Török Á (2002) Oolitic limestone in polluted atmospheric environment in Budapest: weathering phenomena and alterations in physical properties. In: Siegesmund S, Weiss T, Vollbrecht A (eds) Natural stones, weathering phenomena, conservation strategies and case studies. Geological Society, London, Special Publications 205:363–379

Török Á (2003) Surface strength and mineralogy of weathering crusts on limestone buildings in Budapest. Build Environ 38:1185–1192

Török Á (2005) Gypsum-induced decay on the limestone buildings in the urban environment of Budapest. Int J Restor Build Monum 11:71–78

Török Á (2006a) Hungarian travertine: weathering forms and durability. In: Fort R, Alvarez de Buego M, Gomez-Heras M, Vazquez-Calvo C (eds) Heritage weathering and conservation, Taylor & Francis/Balkema, London, vol I:199–204

Török Á (2006b). Black crusts on travertine: factors controlling development and stability. Build Environ (in press)

Török Á, Rozgonyi N (2004) Mineralogy and morphology of salt crusts on porous limestone in urban environment. Environ Geol 46:323–339

Török Á, Siegesmund S, Müller C, Hüpers A, Hoppert M, Weiss T (2006). Differences in texture, physical properties and microbiology of weathering crust and host rock: a case study of the porous limestone of Budapest (Hungary). In: Prikryl R, Smith BJ (eds) Building stone decay. Geological Society Special Publications, London (in press)

Viles HA (1994) Observations and explanations of stone decay in Oxford, UK. In: Thiel MJ (ed) Conservation of stone and other materials, vol I, Causes of disorders and diagnosis. E & FN Spon—RILEM, London, pp 115–120

Winkler EM (1970) The importance of air pollution in the corrosion of stone and metals. Eng Geol 4:327–334

Warscheid T, Braams J (2000) Biodeterioration of stone: a review. Int Biodeterior Biodegradation 46:343–368